Supplementary Information (SI) for Physical Chemistry Chemical Physics.

Supporting Information:

Like-Charge Anion Pairing as a Mechanism for Ion Co-Localization in Charged Aqueous Droplets

Han Nguyen and Styliani Consta*

Department of Chemistry, The University of Western Ontario, London, Ontario, Canada N6A 5B7

E-mail: sconstas@uwo.ca

S1. Force field parameters for OH^-

Table S1: Parameters for the OH^- force field. First and second line show the O and H parameters[S1] in TIP3P-CHARMM. Third and fourth line shows parameters in TIP4P/2005 for a scaled-charge model.[S2] The O-H distance of OH^- is set to 0.98 Å in both TIP3P-CHARMM and TIP4P/2005. ϵ_{LJ} denotes the depth at the minimum of the Lennard-Jones (LJ) potential energy function. $R_{LJ}/2$ is reported instead of σ (size of the atomic site) in the LJ potential energy function as it is used in the CHARMM force field. It is noted that $R_{LJ} = 2^{1/6}\sigma$.

Atomic site	Partial charge [e]	ϵ_{LJ} [kcal/mol]	$R_{LJ}/2$ [Å]
O (in TIP3P-CHARMM)	-1.32	-0.1200	1.7000
H (in TIP3P-CHARMM)	0.32	-0.0460	0.2245
O (in scaled)	-1.2181	-0.060	2.048493
H (in scaled)	0.4681	-0.044	0.809856

S2. Characterization of the droplet's shape fluctuations using the moment of inertia

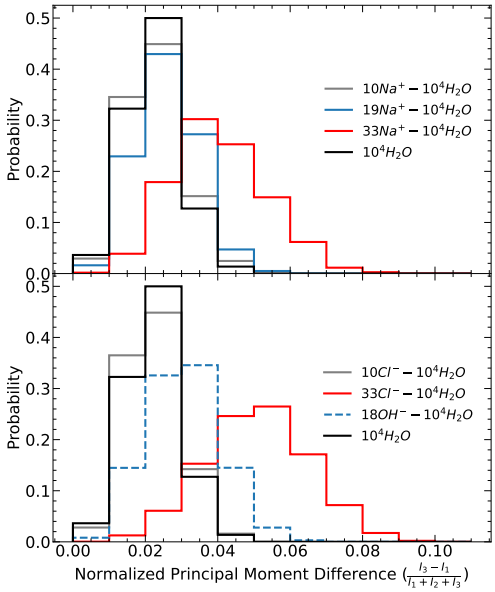

Figure S1: Probability distribution of the ratio of the difference between the largest (I_3) and smallest (I_1) moments of inertia of the droplet divided by the sum of the three moments of inertia ($I_1 + I_2 + I_3$) at 300 K. Upper panel: Na^+ in a droplet with $N_{H_2O} \approx 10^4$. Lower panel: Cl^- and OH^- in $N_{H_2O} \approx 10^4$. A pristine droplet comprised $N_{H_2O} \approx 10^4$ is the reference system.

The profiles shown in Fig. 2 in the main text mask the average depth of the ions from the surface because the shape fluctuations are accounted in an average way. In Fig. S1 shape fluctuations are quantified by the ratio of the difference between the largest (I_3) and smallest (I_1) moments of inertia divided by the sum of the three moments of inertia ($I_1 + I_2 + I_3$) for positive (upper pannel) and negative ions (lower pannel) in $N_{H_2O} \approx 1.0 \times 10^4$. Charged droplets exhibit enhanced shape fluctuations relative to pristine droplets, reflecting the competition between electrostatic repulsion and surface tension. The larger shape fluctuations of the charged droplets is not due to the ion size because the number of H_2O molecules in the charged droplet is decreased relative to a pristine droplet by a number equal to the number of ions. When a $N_{H_2O} \approx 1.0 \times 10^4$ droplet contains $\lessapprox 19$ Na^+ ions, which corresponds to $X \lessapprox 0.33$, the shape fluctuations become very near those of a pristine

H_2O droplet. A charged droplet with 18 OH^- ions (lower pannel in Fig. S1) shows larger fluctuations than the sodiated counterpart (upper pannel in Fig. S1) because of the lower surface tension of the TIP3P-CHARMM modeled droplets than of the TIP4P/2005 model. The negatively charged droplets with 33 Cl^- ions (lower pannel in Fig. S1) show slightly larger fluctuations that the sodiated charged droplets with the same number of ions. This difference may originate from two factors: (i) the different depth of ions from the surface or (ii) different surface tension induced on the droplet by the ions. In previous research[S3] where we used TIP4P/2005 and OPLS ion set of parameters as in the present study, we found that Na^+ and Cl^- have on the average almost the same distance from the droplet's R_e and on the average both maintain their first solvation shell at the surface region as when they are located in the interior. The difference in the solvation shows in the second solvation shell: the number of the H_2O molecules in the second solvation shell of Cl^- ions at the subsurface is reduced more than that of the Na^+ ions relative to their corresponding values in the interior. Therefore, the Cl^- ions appear on the average to be nearer the surface than the Na^+ ions (here we should also consider that the Cl^- has a larger size than the Na^+ ion, therefore, the center of charge for Cl^- is approximately 1.0 Å deeper from the surface relative to a Na^+ ion if we consider that they are both surrounded by a single solvation shell on the surface; however, in terms of depth from the surface the effect of a H_2O layer is larger than that of the size of the ion).

Since the Cl^- ions are slightly nearer the surface they may have reduced electrostatic repulsion and then cause smaller shape fluctuations. The reverse effect observed here may imply that the Na^+ and Cl^- ions affect the droplet's surface tension differently. It is noted that the depth of the ions from the droplet's surface is more clearly differentiated when a polarizable model is used as we have shown in previous work.[S3] The effect of the nature of the ion in the shape fluctuations is not captured in the Rayleigh model and other analytical theories.

The narrower distribution of fluctuations in $N_{Na^+} = 19$ relative to $N_{Na^+} = 33$ is the

reason that the radial ion distribution in Fig. 2 (b) in the main text appears to be shifted to a shorter distance from the droplet's COM relative to that of 33 Na^+ ions at 300 K. In reality the average depth of the Na^+ ions from the surface is the same in both droplets with different net charge.

In microdroplets the difference of the shape fluctuations between the charged and neutral droplets when $X < 1$ will be less pronounced than in the small nanodroplets studied here.

The broader range of shape fluctuations in charged droplets may be associated with larger vapor-liquid interface, and different configurations of the ions and H_2O molecules that may affect the electric field and thus, open new channels for chemical reactions.

S3. Orientation of the H_2O molecules in droplets

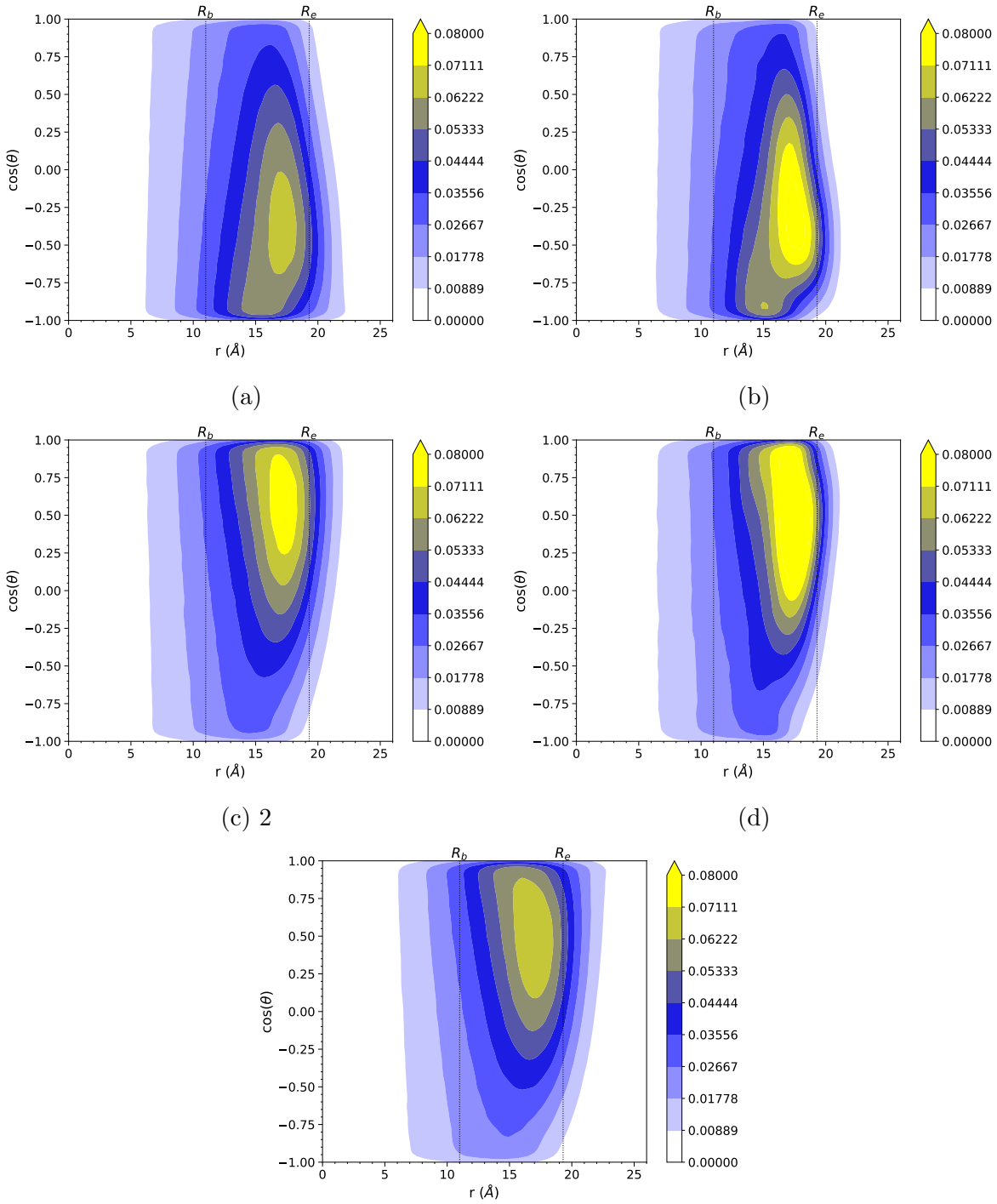

Figure S2: Contour maps of $\cos(\theta)$ distribution of H_2O dipole orientations within successive spherical shells centered at droplet's COM of $N_{H_2O} \approx 10^3$ H_2O and $N_{Na^+} = 8$ at (a) $T = 300$ K and (b) $T = 200$ K. (c) and (d) same as (a) and (b), respectively but for $N_{Cl^-} = 8$. (e) $N_{H_2O} \approx 10^3$ H_2O and $N_{OH^-} = 8$ at $T = 300$ K.

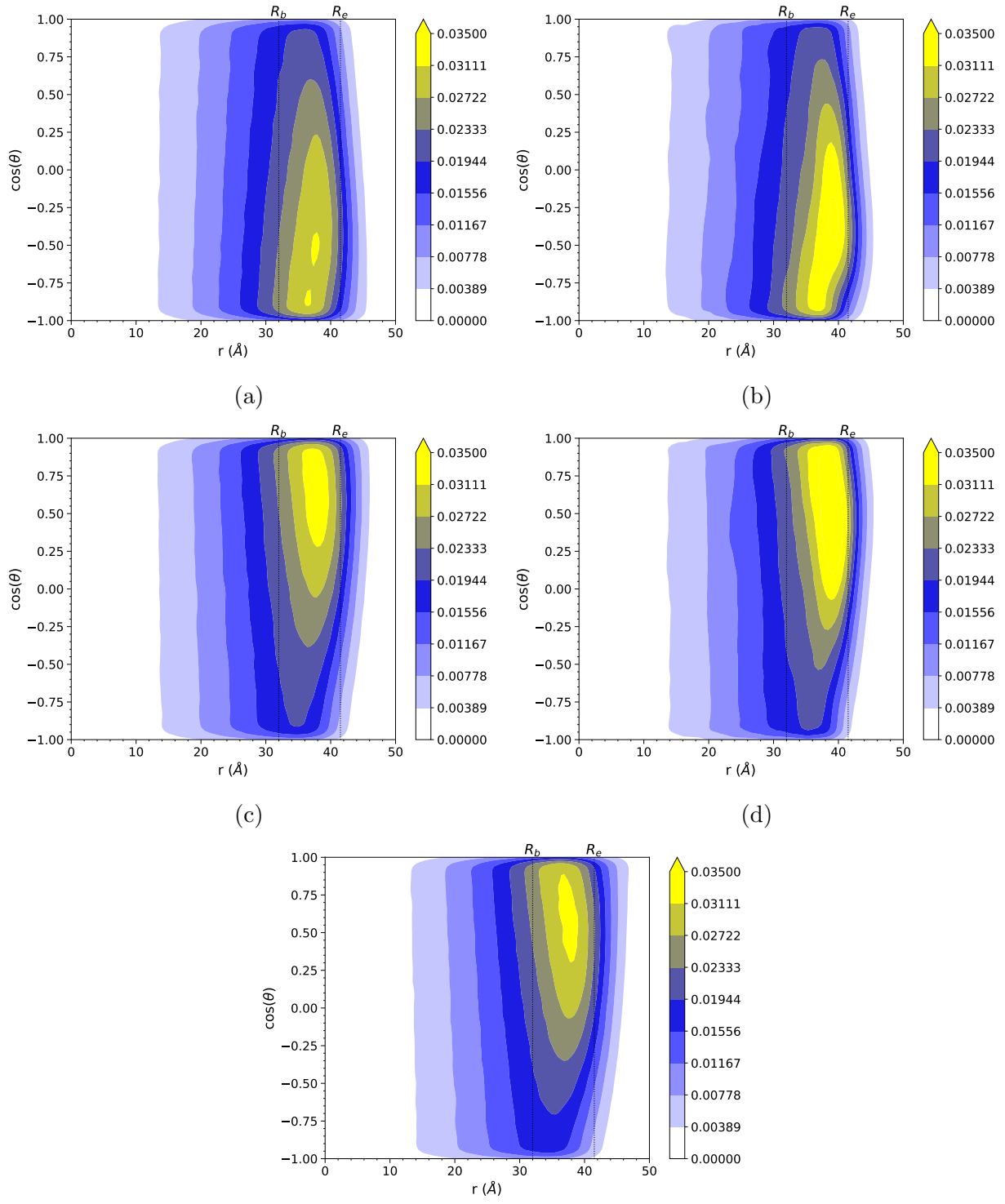

Figure S3: Same as Fig. S2 but for different droplet size. (a) $N_{H_2O} \approx 10^4$ and $N_{Na^+} = 33$ $T = 300$ K and (b) same as (a) at $T = 200$ K. (c) and (d) same as (a) and (b), respectively but for $N_{Cl^-} = 33$. (e) $N_{H_2O} \approx 10^4$ H_2O and $N_{OH^-} = 33$ at $T = 300$ K.

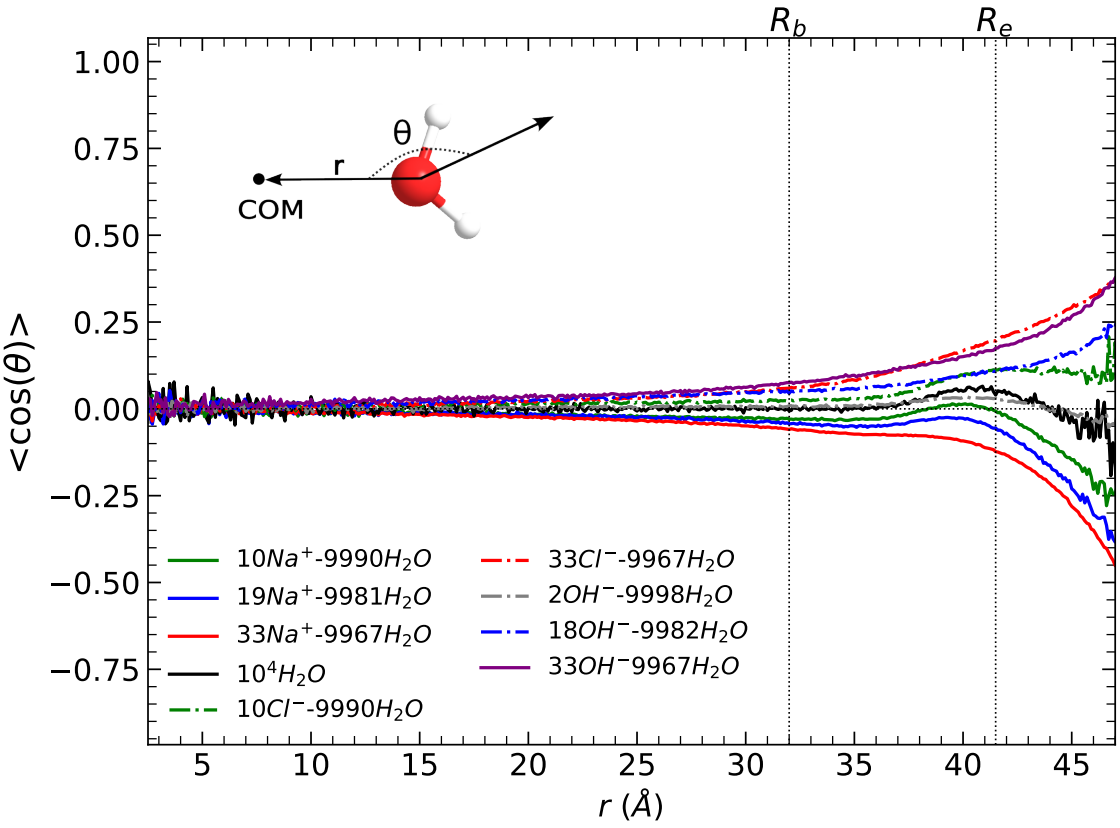

Figure S4: Average $\langle\cos(\theta)\rangle$ as a function of distance (r) from $N_{\mathrm{H_2O}} \approx 10^4$ droplet's COM. Vertical dashed lines mark the R_b and R_e boundaries. The θ angle is defined between the dipole moment of a H_2O molecule defined from the negative site to the positive site and a unit vector from the oxygen site of a H_2O molecule to the droplet's COM.

The orientation of the H_2O dipoles in charged droplets has been studied in our previous research.[S4–S6] Here, we examine possible differences in the orientation of the H_2O molecules in the presence of multiple OH^- ions relative to Cl^-. For completeness, we also include the H_2O orientation in the presence of Na^+ ions. The dipole moment of a H_2O molecule is defined from the oxygen site to the center of the distance between the hydrogen sites. In the orientation contour maps that we present (Fig. S3 and Fig. S3), the angle θ is defined between the H_2O dipole moment and a unit vector from the oxygen site of a H_2O molecule to the droplet's center of the mass (COM). At $T = 300$ K the thermal motions interfere with the effect of the interface and of the net charge in the H_2O orientation. In order to reduce the effect of the thermal motions, simulations were also performed at 200 K. The contour plots of the H_2O dipole orientations at 300 K and 200 K are shown Fig. S3 and Fig. S3 for different droplet sizes.

For all the systems the strongest H_2O dipole orientation is in the surface zone ($R_v < r < R_e$, which has a thickness of ≈ 3 Å) and in the subsurface region ($R_b < r < R_v$) (the surface and subsurface thickness is ≈ 1 nm). The distinct orientation in these regions is expected because this is where the maximum of the ion radial distribution is found. At 200 K the probability of the H_2O molecule orientations for $\cos\theta < 0$ for Na^+ ions and $\cos\theta > 0$ for Cl^- is more uniform in a broader range of angles than at 300 K. At 300K for Cl^- and OH^- ions the H_2O orientations with $\cos\theta$ nearer to $+1$ are more probable than for -1 for the Na^+ ions. We think that this is because of the larger fluctuations of the negative ions as discussed in the previous section. The broader distribution of the OH^- toward the droplet's interior is reflected to a more pronounced orientation of the H_2O molecules penetrating the droplet's bulk-like interior.

It is observed that at $T = 300$ K there is stronger orientation of the H_2O molecules beyond R_e than at $T = 200$ K. We attribute that to the fact that when the fluctuations are larger, there are more H_2O molecules further away from the main body of the droplet. These H_2O molecules are under the influence of the electric field of a spherical droplet that orients

them. Moreover, in the larger fluctuations there are ions that are surrounded by only one solvation shell of H_2O, which is strongly oriented.

Fluctuations in the orientation of the H_2O molecules and of the location of the ions will give rise to instantaneous electric fields, which in turn may affect the chemical reactivity.

The slightly larger shape fluctuations found for Cl^- relative to Na^+ is also evident in the orientation of the H_2O molecules. There is a more pronounced orientation of the H_2O dipoles in the subsurface, surface region and even at $r > R_e$ in the presence of Cl^- and OH^- than of Na^+ ions.

In summary, the strong orientation of the H_2O dipoles in the subsurface and surface region shown in the contour plots arises from the H_2O molecules surrounding the ions. The orientation of the of the outer H_2O molecules beyond R_e is affected by the interface.

S4. Like-charges ion pairing

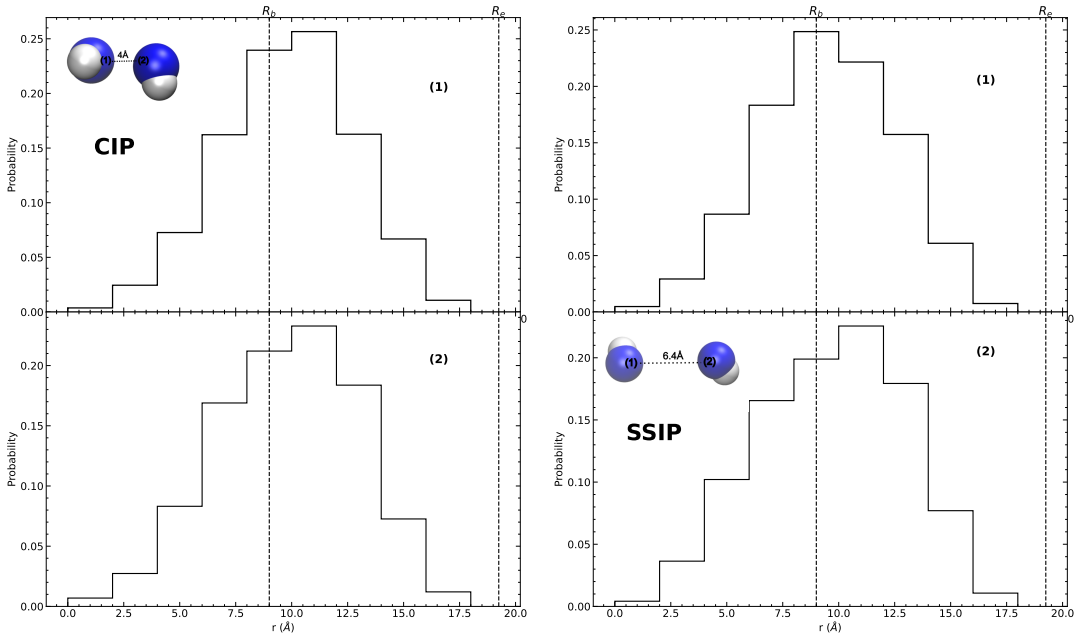

(a) (b)

Figure S5: Probability distribution of the distance of each OH^- ion from the COM of a droplet composed of $N_{H_2O} \approx 10^3$ molecules and 2 OH^- ions when they are (a) in the contact ion-pair (CIP) and (b) in the non-CIP form at $T = 300$ K. The numbers 1 and 2 in the figure denote each of the ions.

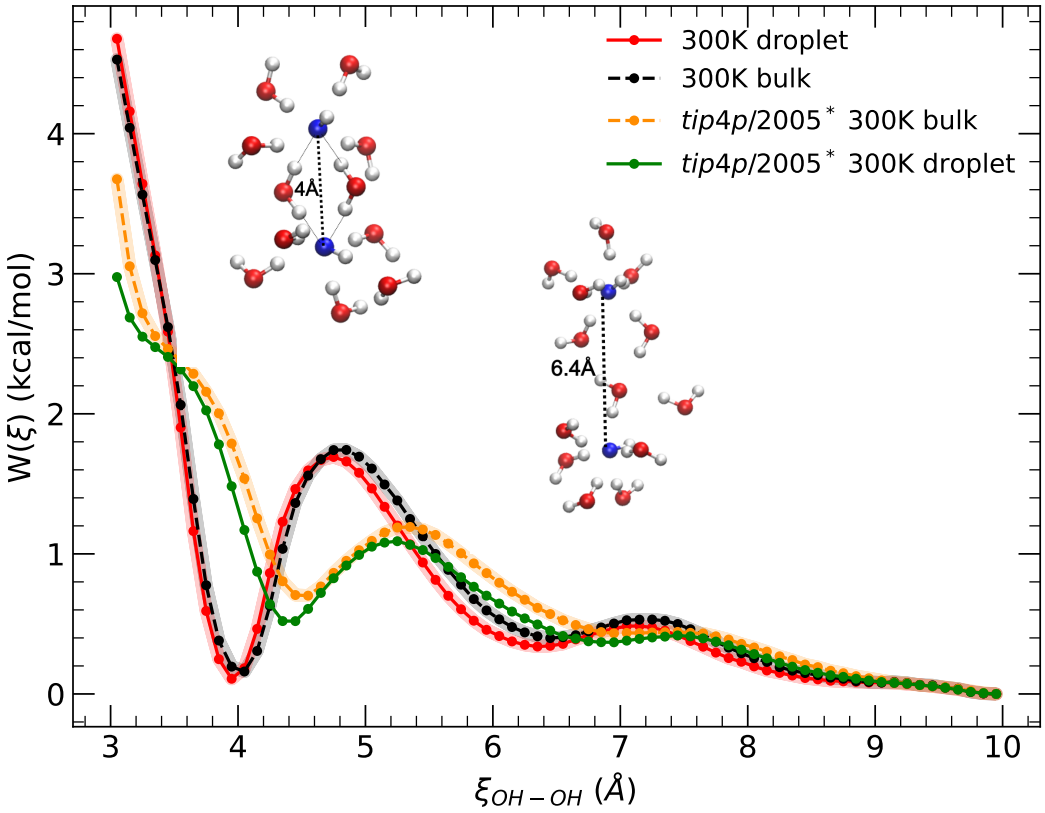

Figure S6: Same as Fig. 4 in the main text where the PMFs are compared using two different force fields. The force fields are: (a) TIP3P-CHARMM water model with OH^- parameters from Ref.;[S7] (b) TIP4P/2005 with scaled charge model from Ref.[S2] denoted by an asterisk in the legend.

S5. Diffusion dynamics

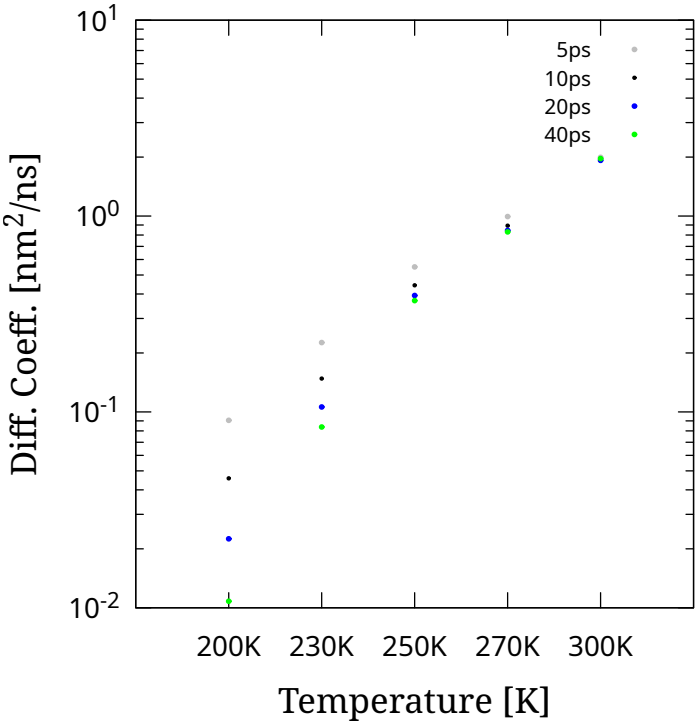

Figure S7: Diffusion coefficients in the droplet interior as a function of temperature at time intervals 5 ps, 10 ps, 20 ps, and 40 ps. The data show that in the temperature range of 230 K-300 K at 40 ps the values of the diffusion coefficient at the droplet's interior have converged.

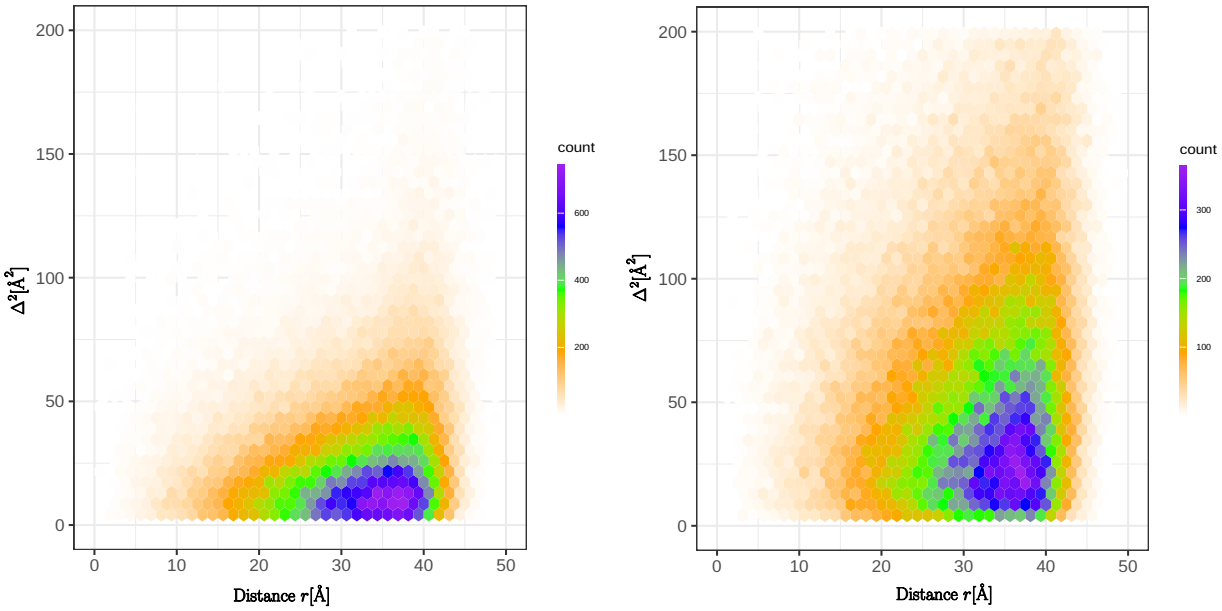

Figure S8: Examples of the distribution of the displacements squared (Δ^2) of the H_2O molecules as a function of the distance from the droplet's COM of a droplet composed of $N_{H_2O} \approx 10^4$ molecules at (a) $T = 270$ K, and (b) $T = 300$ K. The Δ^2 values are computed over 40 ps.

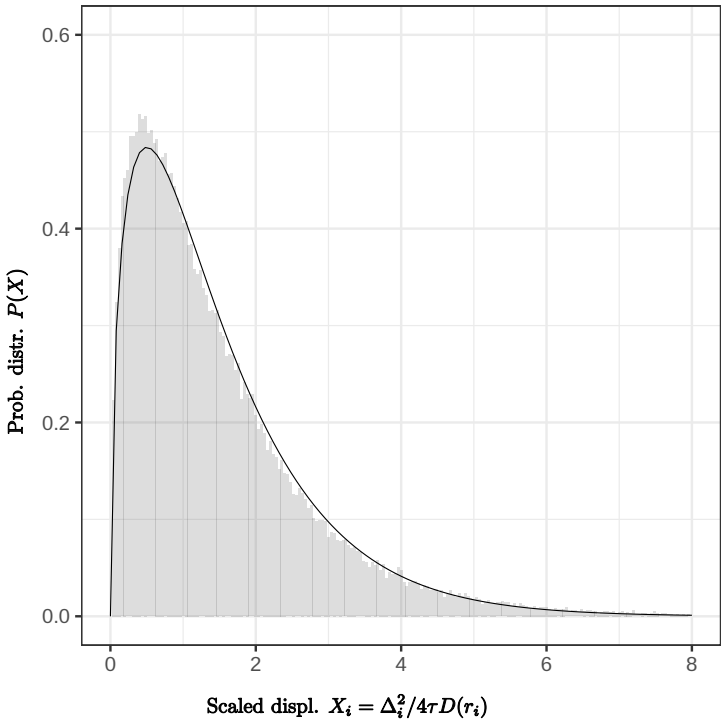

Figure S9: Comparison between the computed probability distribution of the displacements squared (gray bars) with the gamma distribution (solid line), which is the theoretical prediction. Possible sources of any discrepancy are: the diffusion coefficient dependence has more complex dependence on r than that we assumed in the model, and, the diffusion can be anisotropic close to the surface due to pronounced droplet shape fluctuations.

References

(S1) Jorgensen, W. L.; Chandrasekhar, J.; Madura, J. D.; Impey, R. W.; Klein, M. L. Comparison of simple potential functions for simulating liquid water. *J. Chem. Phys.* **1983**, *79*, 926–935.

(S2) Habibi, P.; Rahbari, A.; Blazquez, S.; Vega, C.; Dey, P.; Vlugt, T. J. H.; Moultos, O. A. A New Force Field for OH– for Computing Thermodynamic and Transport Properties of H2 and O2 in Aqueous NaOH and KOH Solutions. *J. Phys. Chem. B* **2022**, *126*, 9376–9387.

(S3) Kwan, V.; Consta, S. Conical shape fluctuations determine the rate of ion evaporation and the emitted cluster size distribution from multicharged droplets. *J. Phys. Chem. A* **2022**, *126*, 3229–3238.

(S4) Kwan, V.; Malevanets, A.; Consta, S. Where do the ions reside in a highly charged droplet? *J. Phys. Chem. A* **2019**, *123*, 9298–9310.

(S5) Kwan, V.; Consta, S. Molecular characterization of the surface excess charge layer in droplets. *J. Am. Soc. Mass. Spectrom.* **2020**, *32*, 33–45.

(S6) Kwan, V.; Consta, S. Bridging electrostatic properties between nanoscopic and microscopic highly charged droplets. *Chem. Phys. Lett.* **2020**, *746*, 137238.

(S7) Chandrasekhar, J.; Spellmeyer, D. C.; Jorgensen, W. L. Energy component analysis for dilute aqueous solutions of lithium (1+), sodium (1+), fluoride (1-), and chloride (1-) ions. *J. Am. Chem. Soc.* **1984**, *106*, 903–910.